Formulation of peptide-based cancer vaccines

Heuts, J.M.M.

CHAPTER 7

Liposomal charge of encapsulated peptide vaccines determines antigen retention at the site of injection, time of antigen presentation and magnitude of T-cell activation

Jeroen Heuts[1,2], Jort van der Geest[2], Robert Cordfunke, Natasja Dolezal, Jan Wouter Drijfhout, Wim Jiskoot[2], Koen van der Maaden*[1] and Ferry Ossendorp*[1]

Manuscript in preparation for submission

[1] Department of Immunohematology, Leiden University Medical Centre, P.O. Box 9600, 2300 RC, Leiden, The Netherlands

[2] Division of BioTherapeutics, Leiden Academic Centre for Drug Research (LACDR), Leiden University, P.O. Box 9502, 2300 RA, Leiden, The Netherlands

ABSTRACT

Antigen-loaded cationic liposomes are effective in inducing antigen-specific T-cell responses and therefore of interest for tumor specific immunotherapy. However, the effect of liposomal charge on particle biodistribution and antigen-specific T-cell priming remains unclear. In this work, the mechanisms of action of liposomes as cancer vaccines formulation are explored. Liposomal biodistribution upon intradermal administration of cationic, neutral and anionic liposomes with comparable physicochemical properties was studied. The liposomes were loaded with near-infrared labeled lipopeptides that contained an ovalbumin $CD8^+$ T-cell epitope, allowing both *in vivo* imaging and the monitoring of specific T-cell responses. The cationic liposomes had the longest retention time of both particle and antigen at the site of injection, up to 350 hrs post vaccination, followed by neutral (150 h) and anionic liposomes (50 h). Only formulations containing cationic liposomes with encapsulated antigen were able to induce functional specific $CD8^+$ T-cells, which were able to inhibit tumor outgrowth in all mice. Only 25% of mice vaccinated with empty liposomes admixed with antigen survived a tumor challenge. In addition, cationic liposomes were able to enhance uptake of both antigenic peptide and protein by dendritic cells *in vitro* and antigen presentation was detectable up to 72 hours post incubation. In summary we show that antigen-loaded cationic liposomes mediate prolonged antigen exposure at the site of injection and facilitate prolonged antigen presentation by dendritic cells explaining the superior vaccination efficacy of cationic liposome formulations.

INTRODUCTION

Cationic liposomes have proven to be efficient delivery vehicles for peptide-based cancer vaccines (1-4). Such vaccines consist of processing-dependent synthetic peptides that can comprise tumor-specific cytotoxic ($CD8^+$) and/or helper ($CD4^+$) T-cell epitopes. Positively charged liposomes have shown to be able to encapsulate a wide range of physicochemically-different peptides and, upon intradermal (i.d.) injection, induce potent antigen-specific T-cell responses that can inhibit and clear established tumors (2-6). Multiple mechanisms of action by which cationic nanoparticles increase vaccine immunogenicity have recently been reviewed by us (1) and include: immunostimulating properties (e.g., upregulation of co-stimulatory molecules, induction of cytokine production) (7-9), increased uptake by dendritic cells (DCs)(10-13) and depot formation at the site of injection (SOI)(14-17). However, which role the cationic charge in liposomes play in the induction of tumor-specific T-cells still has many unknowns.

Prior to DC uptake, cationic liposomes interact with (macro)molecules at the site of injection (SOI) and multiple reports have shown depot formation upon i.d., subcutaneous (s.c.) and intramuscular (i.m.) administration of cationic nanoparticles. This depot is most likely formed by complexation of cationic nanoparticles and negatively charged (macro) molecules present in the interstitial fluids. These depots have been linked to increased vaccine efficacy, since they facilitate prolonged antigen exposure to infiltrating antigen presenting cells (15-18). However, not much is known yet about the relation between depot formation and antigen-specific T-cell priming by such a depot. Our earlier studies with peptide-based cationic liposomes show superior tumor-specific T-cell priming when the peptide is encapsulated instead of admixed with cationic liposomes (3, 4) and [Heuts et al. submitted for publication]. When encapsulated the peptide could be entrapped more efficiently in the depot, resulting in prolonged uptake by DCs and ensure co-delivery of both adjuvant, the liposome, and antigen in the same DCs. We suggested that both factors contribute to the efficient induction of tumor-specific T-cells by cationic liposomes loaded with peptide.

DCs play an orchestrating role in the induction of tumor-specific T-cell responses as they engulf and process liposomal cancer vaccines (1, 19-23). After antigen processing the DCs are able to prime naïve T-cells via the presentation of the exogenous derived antigen (e.g., peptide-loaded liposomes) in MHC class I and class II molecules (20-22, 24). Upon adequate stimulation of the DCs T-cell expansion takes place, which is amplified by several immune-stimulating molecules (e.g., cytokines, surface proteins) produced by the DCs. Multiple reports have shown that cationic lipids and polymers stimulate T-cell priming by activation of DCs, resulting in the upregulation of co-stimulatory molecules, induction of cytokine production, and an enhanced antigen presentation (1, 5, 7-9, 15, 25-28). DC have also been shown to continuously present antigen and prime T-cells over prolonged periods of time (23), resulting in robust and effective antigen-specific

immune responses (19, 28-30). In mice prolonged antigen presentation has been shown up to 72 hours post intravenous (i.v.) administration of antigenic proteins and peptide conjugates (29, 30). Upon DC uptake antigen was stored in lysosome-like organelles that facilitate prolonged antigen supply to MHC class I molecules up to several days (23). The prolonged antigen presentation could be a factor contributing to the efficacy of antigen-loaded cationic liposomes.

In this work we report the influence of liposomal charge and antigen encapsulation on biodistribution and T-cell priming *in vivo*. We studied the effect of liposomal charge on the biodistribution profiles of both nanoparticles and (lipo)peptide in detail. The influence of charge on the induction of specific T-cells and their functionality to control a lethal *in vivo* tumor challenge was determined as well. Finally, we analyzed the uptake of peptide loaded cationic liposomes and subsequent antigen storage and presentation by dendritic cells.

2. MATERIALS & METHODS

2.1 Materials

Ovalbumin protein labeled with Alexa 647 was purchased from Thermo Fisher (Bleiswijk, the Netherlands) and the near-infrared dyes IRDye680RD maleimide and IRDye800CW-NHS were obtained from LI-COR Biosciences (Lincoln, USA). The lipids 1,2-dioleoyl-3-trimethylammoniumpropane (DOTAP), 1,2-dioleoyl-sn-glycero-3-phosphocholine (DOPC), 1,2-dioleoyl-sn-glycero-3-phosphoethanolamine (DOPE) and 1,2-dioleoyl-sn-glycero-3-phospho-(1'-rac-glycerol) (DOPG) were purchased from Avanti Polar Lipids (Alabaster, Alabama, USA). Chloroform ($CHCl_3$), methanol (MeOH) and acetonitrile (ACN) were obtained from Biosolve BV (Valkenswaard, the Netherlands). Ammonium hydroxide 25% (w/v) was purchased from Brocacef BV (Maarssen, the Netherlands) and from Sigma Aldrich (Zwijndrecht, the Netherlands) trifluoracetic acid (TFA), NP-40, chlorophenol red-β-galactopyranoside (CPRG), dimethyl sulfoxide (DMSO) and 50 μM β-mercaptoethanol (2-βME) were obtained. Vivaspin 2 centrifuge membrane concentrators from Sartorius Stedim Biotech GmbH *(*Göttingen, Germany*)*. Iscove's modified Dulbecco's medium was purchased from Lonza (Lonza Verniers, Belgium) and fetal calf serum from Greiner Bioscience (Alphen a/d Rijn, the Netherlands). Glutamax, glutamin and penicillin/streptomycin were obtained from Thermo Fisher (Bleiswijk, the Netherlands) and 80 IU/ml sodium-penicillin G from Astellas (Leiden, the Netherlands). Hygromycin B (500 μg/ml) from AG Scientific (San Diego, USA). Paraformaldehyde and fluorescent labeled antibodies for CD8 and CD3 for flow cytometry analysis were obtained from BioLegend (London UK). The fluorescent labeled SIINFEKL specific MHC class I tetramer was produced by the peptide facility of the Department of Immunology at the Leiden University Medical Center (LUMC). Phosphate buffers were composed of 7.7 mM $Na_2HPO_4 \cdot 2\ H_2O$ and 2.3 mM $NaH_2PO_4 \cdot 2\ H_2O$, pH 7.4 (10 mM PB, pH 7.4) in deionized water with a resistivity of 18 MΩ•cm, produced by a Millipore water purification system (MQ water).

The PB buffer was filtered through a 0.22 μm Millex GP PES-filter (Millipore, Ireland) prior to use.

2.2 (Lipo)peptide and fluorescent lipid synthesis

All synthetic peptides and lipopeptides were synthesized and purified at the peptide facility of the Department of Immunology at the LUMC. Lipopeptides were composed of the OVA24 peptide (table 1), containing the ovalbumin derived SIINFEKL epitope, and a lipid tail (stearyl on the N-terminus of the OVA24 peptide by hot solid phase peptide synthesis. The OVA24-stearyl was then purified by preparative HPLC on a Jasco HPLC system equipped with a C4 column with a flow rate of 4 ml/min. Identification was performed by MALDI-TOF and final quantification was done by measuring the absorbance at 214 nm. To prepare fluorescent (lipo)peptides, first OVA24-C with and without stearyl were synthesized, whereby the glutamic acid of the OVA24 sequence was replaced by a cysteine. Subsequently, the near-infrared label IRDye680RD-maleimide was covalently coupled to the cysteine of the OVA24-C (lipo)peptide (table 1). Fluorescent DOPE was prepared by covalent attachment of the near-infrared label IRdye800CW-NHS to the primary amine in the polar part of DOPE in methanol for one hour at 30˚C. Subsequently, the unattached dye was removed from the reaction mixture by performing a Bligh-and-Dyer extraction (methanol/chloroform/0.1M HCl) 10 times, whereby the water/methanol phase (that contained to non-reacted/free dye) was removed after each repetition (suppl fig. 1). Finally, the DOPE-IRdye800 in the chloroform phase was dried under a stream of nitrogen and was dissolved in methanol. The concentration of DOPE-IRdye800 was determined by measuring the absorbance at 778 nm and using the specific molar extinction coefficient of the dye (according to manufacturer's protocol) and the final ration free DOPE/DOPE-IRdye800 was [3:1], as determined by RP-HPLC.

Table 1. Amino acid sequence of the peptides used in this study. The $CD8^+$ T-cell epitope is indicated in italic and the cysteine to which the near-infrared label is attached is indicated in bold.

Name	Sequence
OVA24	D**E**VSGLEQLE-*SIINFEKL*-AAAAAK
OVA24-IR680	D**C**VSGLEQLE-*SIINFEKL*-AAAAAK
$OVA24_{Stearyl}$	Stearyl- D**E**VSGLEQLE-*SIINFEKL*-AAAAAK
$OVA24_{Stearyl}$-IR680	Stearyl- D**C**VSGLEQLE-*SIINFEKL*-AAAAAK
NBD labeled SIINFEKL	NBD-G-RKDDKDDKDLA-*SIINFEKL*-AAAK

2.3 Liposome formulation

Liposomes loaded with peptide were prepared by the earlier described thin film dehydration-rehydration method (2, 4). In brief, the lipids (table 2) were dissolved in $CHCl_3$ followed by rotary-evaporation to obtain a dry lipid film. The lipid film was rehydrated with a 1 mg/ml solution NBD labeled OVA24 in ACN/MQ (1:1, v/v) or 1 mg/ml solution of the full ovalbumin protein admixed with it's Alexa 647 labeled analog (weight ratio

1:0.1). The resulting dispersion was snap-frozen followed by overnight lyophilization in a Christ alpha 1-2 freeze dryer (Osterode, Germany). Lipopeptide-loaded liposomes were prepared by adding the lipopeptide (dissolved in MeOH) to the lipid mixtures (in $CHCl_3$) followed by rotary evaporation to obtain a dry lipid film. For all formulations the dry lipid cake or dry lipid film was rehydrated with PB in three consecutive steps: twice the addition of 25% of the final volume (30 minutes equilibration after each addition) and as a third step the remaining 50% of the final volume was added (followed by 1 hour equilibration). All liposomes formulations were down-sized by extrusion with a Lipex extruder (Northern Lipids Inc., Canada), the particles were extruded four times through a 400 nm and four times through a 200 nm polycarbonate filter (Nucleopore Milipore, Kent, UK). Finally the peptide-loaded liposomes were purified and concentrated by making use of Vivaspin 2 centrifugation concentrators (molecular-weight-cut-off of 300 kDa), as described previously (2, 4). The liposomal dispersions were concentrated 5-fold by centrifugation at 931 g (2000 rpm). Subsequently, the formulations were re-diluted with PB to its initial volume after which the concentration step was repeated. During purification, samples of the liposomal fraction and the flow-through were taken to determine free and encapsulated peptide, as described below.

Table 2. Composition and method of preparation of the liposomal formulations used in this study

Formulation	Cargo	Cargo amount (μM)	DOTAP (mM)	DOPC (mM)	DOPG (mM)	DOPE-IR_{800} (mM)
(+) Liposomes [Pep]	OVA24	393	6.74	6.74	n.a	n.a
(+) Liposomes [Lipopep]	OVA24-stearyl	393	6.74	6.74	n.a	n.a
(0) Liposomes [Lipopep]	OVA24-stearyl	393	n.a.	13,48	n.a	n.a
(-) Liposomes [Lipopep]	OVA24-stearyl	n.a.	n.a.	6.74	6.74	n.a.
Fluorescent liposomes						
(+) Liposomes-IR_{800}	n.a.	n.a.	6.74	6.74	n.a	0.125
(+) Liposomes [Pep-NBD]	NBD labeled SIINFEKL	393	6.74	6.74	n.a	n.a.
(+) Liposomes [Prot.Alexa648]	Ovalbumin Alexa fluor 647	393	6.74	6.74	n.a	n.a.
(+) Liposomes-IR_{800}	n.a.	n.a.	6.74	6.74	n.a	0.125
(+) Liposomes-IR_{800} [Lipopep-IR_{680}]	OVA24-stearyl-IR_{680}	393	6.74	6.74	n.a	0.125
(0) Liposomes-IR_{800} [Lipopep-IR_{680}]	OVA24-stearyl-IR_{680}	393	n.a.	13.48	n.a	0.125
(-) Liposomes-IR_{800} [Lipopep-IR_{680}]	OVA24-stearyl-IR_{680}	393	n.a.	6.74	6.74	0.125

2.4 Physicochemical properties of liposomal formulations

The hydrodynamic diameter (Z-average) and the polydispersity index (PDI) were determined by using dynamic light scattering (DLS). The zeta-potential was determined by using laser Doppler electrophoresis. Both measurements were performed on a Zetasizer Nano (Malvern Instruments, Malvern, UK) and prior to analysis the samples were diluted 100 fold in PB. The physicochemical properties of all liposomal formulations were determined at several time points form the day of production until 8 weeks after production to determine liposome stability.

2.5 (Lipo)peptide quantification by RP-UPLC-UV

The recovery of the (lipo)peptide in the liposomal formulations was determined by RP-UPLC-UV analysis (Waters Acquity UPLC[å] combined with an Acquity UV detector and a Waters BEH C18 – 1.7 mm (2.1 ´ 50 mm) column). An ACN/MQ with 0.1% TFA gradient with a flow rate of 0.5 ml/min was used. The run was initiated with 95% solvent A (MQ water with 0.1% TFA) and 5% solvent B (ACN with 0.1% TFA) followed by a linear gradient to 100% solvent B in 7 minutes staying at 100% B until 9 minutes and back to the initial 5% solvent A at 9.1 minutes. (Lipo)peptides were detected by measuring the UV absorbance at λ = 214 nm. Liposomal samples were diluted 20-fold in 1:1 (v/v) MeOH:MQ water prior to injection on the UPLC system. Calibration curves for both peptides were prepared by automated injections of increasing volumes (5-50 μL) from a 50 μg/ml (lipo)peptide solution in 1:1 (v/v) MeOH:MQ water. Quantification was done by integration of the peptide peaks to obtain the area under the curve (AUC) of all calibration samples, based on the AUC linear calibration curves were fitted. The AUC of the (lipo)peptide peaks in the samples was determined by peak integration using MassLynx software (Waters, software 4.2.) and was followed by interpolation of the AUCs and standard curve by interpolation using Graphpad prism 8.

2.6 Lipid quantification by RP-UPLC-ELSD

Lipid recovery was determined by using the same RP-UPLC-UV system coupled to a Waters ACQUITY UPLC® ELS Detector. The same gradient method was used as described under 2.5. Liposomal samples were diluted 100-fold in 1:1 (v/v) MeOH:MQ water prior to injection of 10 μL, and calibration curves for DOTAP, DOPC, DOPG and DOPE-IR_{800} were prepared by automated injections of increasing volumes of 5-50 μl from a 50 μg/mL lipid stock solutions in 1:1 (v/v) MeOH:MQ water solution. Quantification was done by integration of the lipid peaks to obtain the AUC of all calibration samples. Based on the AUCs, calibration curves were fitted by second order polynomial regression. The AUC of the lipid peaks in the samples determined by integration was determined by interpolation of sample AUC on the corresponding lipid calibration. Peak integration and interpolation was done by using MassLynx software (Waters, software 4.2.) and interpolation by using Graphpad prism 8.

2.7 *In vivo* imaging

To investigate the influence of liposomal charge on the residence time at the site of injection and biodistribution live imaging using the IVIS spectrum (Perkinelmer) was performed. For the biodistribution studies albino C57BL/6 (B6/Rj-Tyr$^{c/c}$) were obtained from Janvier labs (Le Genest-Saint-Isle, France). Experiments started when the mice were 8 – 12 weeks old and all studies were carried out under the guidelines of the animal ethic committee of the Netherlands. Mice were (i.d.) injected with the compounds in a total volume of 30 μL of PBS.

2.8 Prophylactic vaccination studies of liposomal formulations in vivo

In order to study the influence of liposomal charge on CD8$^+$ T-cell priming a prophylactic tumor experiment was performed. The in vivo induction of SIINFEKL CD8+ T-cells in blood was determined in mice immunized (i.d.) at the tail base. All mice were vaccinated with 10 nm of liposomal or free (lipo)peptide on day 0 (prime) and day 14 (boost). Blood samples were obtained from the tail vein at multiple timepoints after which red blood cell lysis was performed. The remaining cells were stained with fluorescently labeled antibodies against CD8, CD3 and the MHC class I Kb tetramers presenting the SIINFEKL peptide epitope. Live and dead cells were distinguished by using the 7-AAD viability staining solution. Cells were analyzed with the BD LSR-II flow cytometer and data was analyzed by making use of the Flowjo software. At day 32 mice were s.c. injected in the flank with 1x10^5 B16 tumor cells in 200 μL PBS and tumor size was measured 2 to 3 times per week by making use of a caliper. Mice were euthanized when tumor volume exceeded 1500 mm^3.

2.9 Antigen uptake and prolonged storage

To determine the effect of liposomal encapsulation on antigen uptake and storage the immortalized murine dendritic cell line D1 were incubated with plain or liposome-loaded peptide or protein. The DCs were incubated for 2.5 hours with nitrobenzoxadiazole (NBD) labeled SIINFEKL (4 μM) (table 1) or OVA-Alexa647 (0.1 μM) as free compound or encapsulated in cationic liposomes. DCs were washed with IMDM and cultured for 0, 24, 48 or 72 hours. Next, the cells were washed in staining buffer (PBS + 0.1% (w/v) bovine serum albumin (BSA) + 0.05% (w/v) sodium azide) and fixated for 30 minutes in 0.5% paraformaldehyde. Finally, the DCs were measured on a LSR-II flow cytometer (BD Bioscience, San Jose, CA) to determine the peptide or protein uptake and storage. Data were analyzed with FlowJo software v10.6.1.

2.10 *In vitro* antigen presentation

The *in vitro* antigen presentation by D1 dendritic cells was monitored up to 72 hours post incubation to study antigen presentation of liposomal antigen compared to plain antigen. The D1 cells were incubated with 2 μM of either plain peptide or peptide formulated in liposomes in IMDM (supplemented with 7.5 % fetal calf serum, 2 mM Glutamax and 80 IU/ml sodium-penicillin G) and during 2.5 hours at 37 °C and 5% CO_2. Next, cells were

washed with IMDM to remove the excess of formulation and plated on 30 mm dishes (3x10^5 cells/dish) and cultured for 0, 24, 48 or 72 hours. Subsequently, cells were harvested, counted and plated on a 96-well plate (5x10^4 cells/well) and $CD8^+$ T-cell hybridoma B3Z cells ($5x10^4$ cells/well) were added for an overnight co-culture. The B3Z cell line is specific for the H-$2K^b$ –presented SIINFEKL epitope and contains the LAcZ reporter under regulation of NF-AT element of the IL-2 promotor (31). Upon binding of its T-cell receptor with Kb- SIINFEKL complexes on the D1 cell surface β-galactosidase is produced upon T-cell activation. The following day the cells were washed in PBS and incubated with a CPRG-containing lysis buffer (PBS + 1% 18 mg/ml CPRG + 0.9% 1 M MgCl2 + 0.125% NP40 + 0.71% 14.3 M 2-βME) , allowing colorimetric quantification of the enzymatical conversion. The OVA8 peptide containing only the SIINFEKL minimal epitope (100 ng/ml in PBS) was used as positive control and D1 cells loaded with empty liposomes served as negative control. The optical density (OD) was determined with an iMark™ microplate reader at a wavelength of 595 nm.

3.RESULTS

3.1 Physicochemical properties of liposomal formulations

Liposomes varying in charge, antigen cargo and fluorescent label were prepared to study particle behavior and antigen delivery, both *in vitro* and *in vivo* (table 3). All liposomes had comparable hydrodynamic diameters and PDIs, but had different zeta potentials dependent on the lipid composition. The formulations were composed of di-oleoyl lipids, similar to the cationic DOTAP:DOPC liposomes used in our previous studies (2-4, 32, 33). In order to exclude varying peptide loading efficiencies for cationic, neutral and anionic liposomes a lipopeptide was designed containing the processing-dependent ovalbumin derived SIINFEKL $CD8^+$ T-cell epitope (table 1). Encapsulation of the lipopeptide resulted in high encapsulation efficiencies (>90%, as determined by rp-UPLC) irrespective of liposomal charge. Final lipid content of all formulations varied in-between 1 and 5 mM (table 3, suppl. fig 2). The incorporation of $IRdye_{800}$ labeled lipids and $IRdye_{680}$ labeled lipopeptides did not alter liposomal physicochemical characteristics (table 3). Stability of the lipopeptide loaded liposomes was determined up to 8 weeks of storage (2 – 8 °C) and no notable changes in hydrodynamic diameter, polydispersity index (PDI) and zeta-potential were observed for the cationic and anionic liposomes. An increase of hydrodynamic diameter and PDI was observed for the neutral liposomes throughout storage (suppl. fig 3).

Table 3. Physicochemical properties of the prepared liposomal formulations containing di-oleoyl lipids. Formulations were composed of 10 mg/ml of lipids and 1 mg/ml of (lipo)peptide. (+) = cationic, (0) = neutral and (-) = anionic. The loaded (fluorescent) antigen is indicated in between squared brackets. [pep] = peptide, [pep.NBD] = Nitrobenzoxadiazole conjugated peptide, [Prot. AL] = Alexa 648 conjugated ovalbumin protein, [pept.IR] = IR_{dye} conjugated peptide Stearyl indicates the lipopeptide. Data shown as mean ± SD (n=3).

Formulation	Hydrodynamic diameter (nm)	PDI	Zeta-potential (mV)
(+) Liposomes	137.8 ± 2.2	0.13	27.4 ± 0.7
(+) Liposomes [Pep]	144.2 ± 1.0	0.13	25.3 ± 0.14
(+) Liposomes [Lipopep]	131.1 ± 0.3	0.11	23.2 ± 1.1
(0) Liposomes [Lipopep]	160.0 ± 8.4	0.18	-19 ± 0.74
(-) Liposomes [Lipopep]	142.8 ± 0.9	0.17	-47.7 ± 0.24
Fluorescent liposomes			
(+) Liposomes [Pep-NBD]	126.2 ± 1.4	0.14	24.0 ± 0.6
(+) Liposomes [Prot.Alexa648]	185.7 ± 6.3	0.31	33.1 ± 1.2
(+) Liposomes-IR_{800}	194.5 ± 0.6	0.18	32.0 ± 0.9
(+) Liposomes-IR_{800} [Lipopep-IR_{680}]	169.6 ± 1.7	0.22	27.8 ± 1.1
(0) Liposomes-IR_{800} [Lipopep-IR_{680}]	194.5 ± 0.6	0.18	-7.4 ± 0.9
(-) Liposomes-IR_{800} [Lipopep-IR_{680}]	193.5 ± 2.7	0.27	-67.2 ± 0.7

3.2 Effect of liposomal charge on retention at the site of injection and T-cell induction

3.2.1. Antigen and particle retention of antigen-loaded liposomes

The *in vivo* biodistribution of lipopeptide-loaded cationic, neutral and anionic liposomes was determined upon i.d. administration. In order to monitor the behavior of both liposome and peptide IRdye labeled variants of the liposomes and lipopeptides were used (table 3). The lipopeptide formulated in cationic liposomes resulted in the longest retention at the SOI, up to 350 hours post vaccination. When formulated in neutral and anionic liposomes the lipopeptide was detectable at the SOI 150 and 50 hours post vaccination, respectively (fig 1). A similar trend was observed for the liposomal label, with decreasing liposomal charge the retention time at the SOI decreased as well (fig 1). The SOI exposure (sustained presence), determined as the area under the curve (AUC), of both empty and lipopeptide loaded cationic liposomes was significantly higher compared to the neutral and anionic formulations (fig 2).

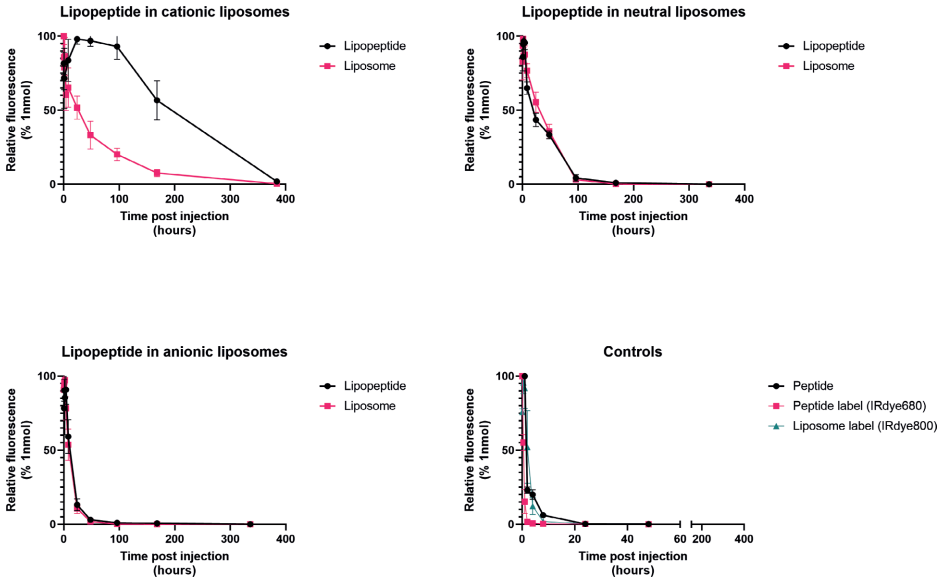

Figure 1. Encapsulation of lipopeptide in cationic liposomes increased retention time at the SOI. Encapsulation in neutral or anionic liposomes did not or minimally extended retention at the SOI. Data shown as mean +/- SD (n=3).

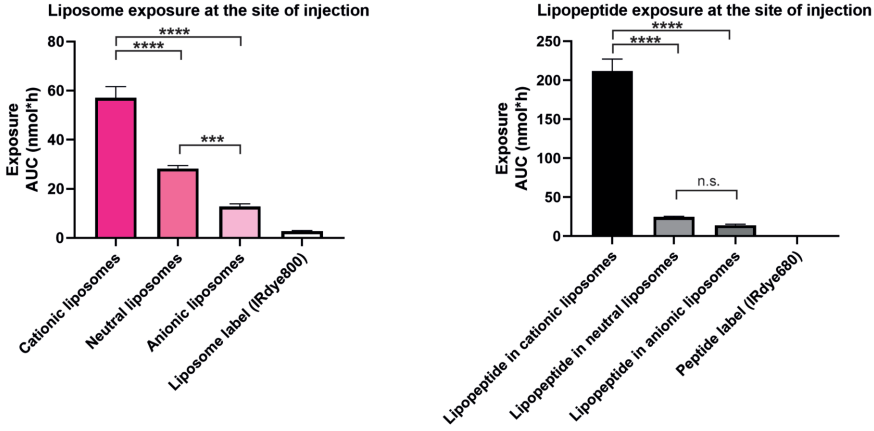

Figure 2. Exposure (sustained presence) of liposomes (left) and lipopeptide (right) at the site of injection after i.d. administration. Exposure was determined by AUC of data shown in figure 1. Cationic liposomes had a significant higher exposure at the SOI compared to neutral and anionic liposomes. The same trend was observed for the encapsulated peptide in these liposomes. Data shown as mean ± SD (n=3) and analyzed by one-way Anova with Tukey's multiple comparisons test. *p < 0.05, ** p<0.01, *** p<0.001, **** p<0.0001.

3.2.2 T-cell induction upon vaccination

The priming and functionality of SIINFEKL specific CD8+ T-cells upon vaccination with (lipo)peptide- loaded cationic, neutral and anionic liposomes was evaluated in mice. Induction of antigen-specific CD8+ T-cells was only observed in mice vaccinated with both cationic liposomes and encapsulated antigen (fig 3). Vaccination with lipopeptide-loaded cationic liposomes induced the highest levels of SIINFEKL-specific CD8+ T-cells and 75% of the vaccinated mice were able to inhibit tumor outgrowth after a lethal tumor challenge. Both neutral and anionic lipopeptide-loaded liposomes did not differ from the control group (plain peptide), no induction of tumor specific T-cells and all mice developed tumors after the tumor challenge (fig. 3). Both neutral and anionic liposomes were able to, moderately, activate SIINFEKL specific CD8+ T-cells *in vitro* (suppl. fig 4). Confirming that both formulations contained functional peptide.

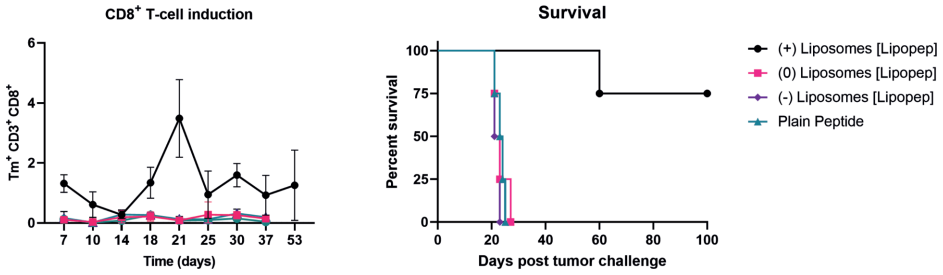

Figure 3. Induction (left) of SIINFEKL-specific CD8 T-cells in peripheral blood upon vaccination with the indicated formulations. SIINFEKL-specific CD8+ T-cells were determined by tetramer staining and flow-cytometry and data is shown as mean± SD. Survival of mice (right) of mice vaccinated with indicated formulations after a challenge with 1x10^5 ova-B16 tumor cells (n=4). All mice were i.d. vaccinated on day 0 and day 14 with 1 nmol of peptide in 30 μL of PBS.

3.3 Effect of antigen encapsulation in cationic liposomes on SOI retention, CD8+ T-cell induction and antigen presentation

3.3.1 Retention of antigenic peptide formulated in cationic liposomes at the site of injection

Next, we studied the effect of antigen loading on antigen retention at the SOI. Therefore, mice were vaccinated with antigenic peptide admixed with or encapsulated in cationic liposomes. The labeled cationic liposomes were detectable at the SOI up to 300 hours post injection (fig. 4). When the OVA_{24}-IR680 was mixed with empty liposomes prior to injection the peptide was detected up to 300 hours post injection at the SOI (fig. 4). Encapsulation of the OVA_{24}-IR680 in labeled liposomes prolonged detection of the peptide up 380 hours post injection at the SOI. Throughout the whole experiment the relative fluorescence at the SOI was highest for the liposomal encapsulated OVA_{24}-IR680 (fig. 4). Liposomes were able to prolong OVA_{24}-IR680 retention at the SOI upon mixing, however, encapsulation prolonged retention of the peptide (fig. 4, 5). The exposure at the

SOI of liposomal loaded peptide was significantly higher compared to peptide admixed with empty liposomes (fig 6). Encapsulation of the peptide also resulted in a higher exposure of the liposomes at the SOI (fig 6).

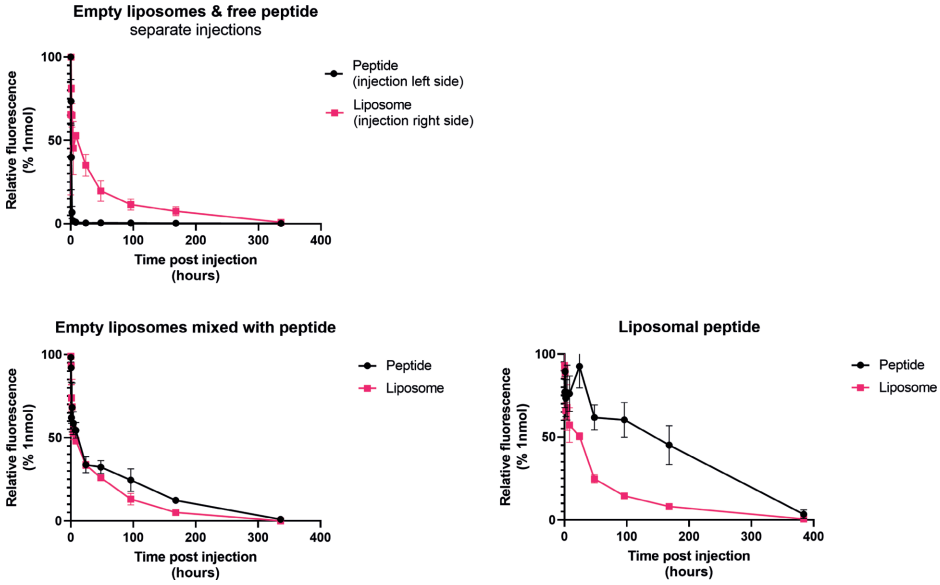

Figure 4. In vivo retention at injection site of fluorescent cationic liposomes and fluorescent peptide (top left) injected separately; fluorescent peptide with empty fluorescent liposomes mixed prior to injection (bottom left) and liposomal encapsulated fluorescent peptide (bottom right). Results shown as mean ± SD (n=3).

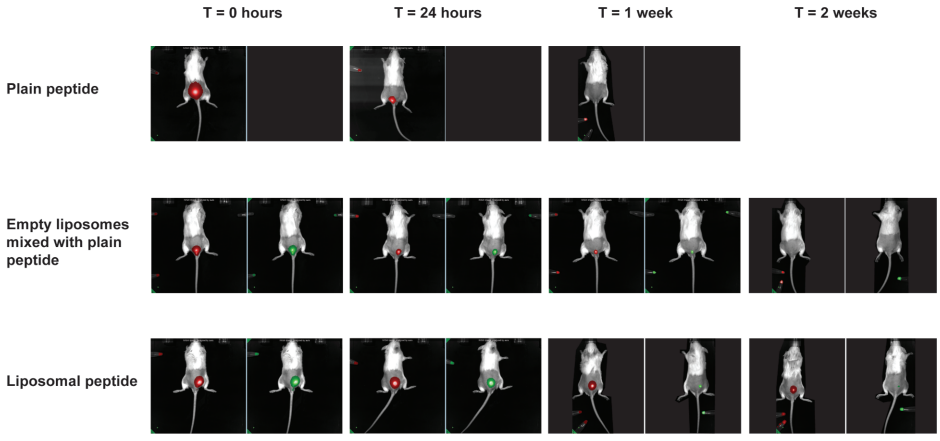

Figure 5. Representative images of mice injected fluorescent peptide (n=3) (left panel, Indicated in red) and/or fluorescent liposomes (n=3) (right panel, indicated in green).

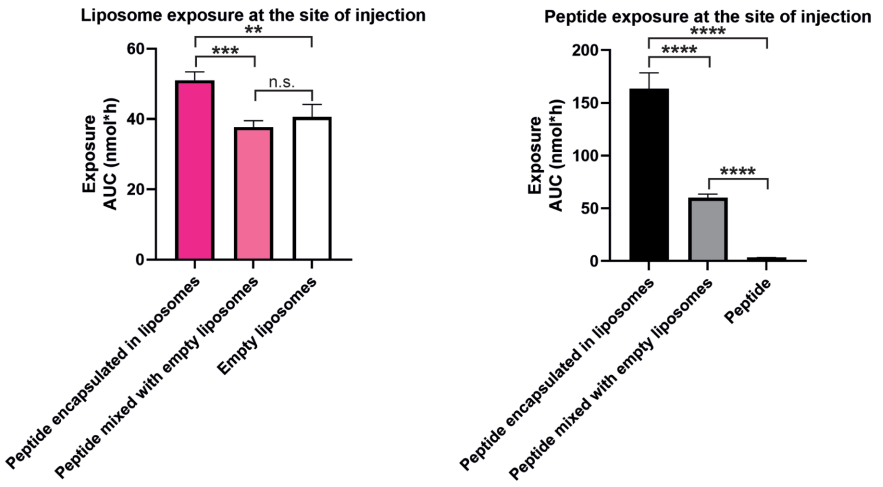

Figure 6. Exposure (sustained presence) of liposomes (left) and peptide (right) at the site of injection after i.d. administration. Peptide encapsulated in cationic liposomes had a significant higher exposure at the SOI compared to peptide admixed with cationic liposomes. Data shown as mean ± SD (n=3) and analyzed by one-way Anova with Tukey's multiple comparisons test. *p < 0.05, ** p<0.01, *** p<0.001, ****p<0.0001.

3.3.2 T-cell induction upon vaccination

The priming and functionality of SIINFEKL specific CD8+ T-cells upon vaccination cationic liposomes loaded with or mixed was evaluated in mice. Vaccination with cationic liposomes loaded with peptide induced the highest levels tumor specific T-cells and protected all mice against tumor outgrowth (fig 7). Plain peptide admixed with cationic liposomes induced lower levels of tumor-specific CD8+ T-cells and only 25% of these mice survived the tumor challenge.

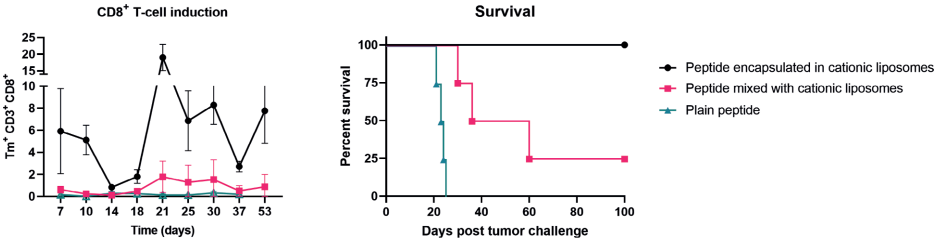

Figure 7. Induction (left) of SIINFEKL-specific CD8 T-cells in peripheral blood upon vaccination with the indicated formulations. SIINFEKL-specific CD8+ T-cells were determined by tetramer staining and flow-cytometry and data is shown as mean± SD. Survival of mice (right) of mice vaccinated with indicated formulations after a challenge with 1x10^5 ova-B16 tumor cells (n=4). All mice were i.d. vaccinated on day 0 and day 14 with 1 nmol of peptide in 30 μL of PBS.

3.3.3 Intracellular storage of antigen-loaded cationic liposomes in dendritic cells

Next, we studied uptake and intracellular storage of peptide- and protein-loaded cationic liposomes in DCs. These antigen-presenting cells are specialized in uptake and handling of several antigen-formulations. Targeting of different receptor mediated uptake routes lead to storage of antigen and sustained antigen processing and presentation (23, 30). A NBD labeled peptide, containing the SIINFEKL epitope, or the full ova protein, labeled with Alexa 648, were loaded in cationic liposomes to track the antigen in live DCs. Both the free peptide and protein did not show detectable uptake by the DC (fig. 8). Liposomal encapsulation enhanced uptake of both the fluorescently labeled peptide and the protein, which is in-line with literature (1, 28, 34). Besides enhanced uptake both the peptide and protein were detected in the DCs for at least 72 hours post incubation (fig 8).

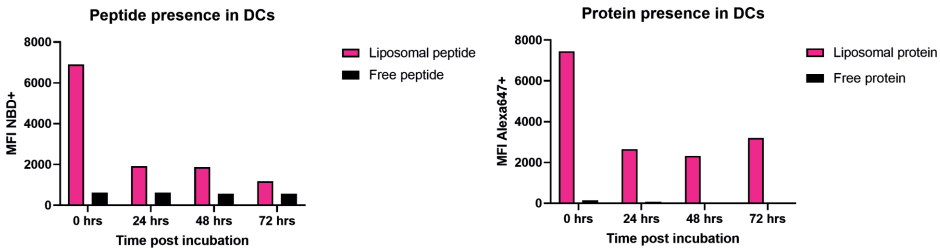

Figure 8. In vitro uptake and sustained storage of cationic liposomal antigenic peptide or protein (2 μM) by DCs. The DCs were loaded with (left) liposomal or free NBD labeled peptide, containing the SIINFEKL epitope, and (right) liposomal or free fluorescently labeled OVA protein (right). Cells were incubated for 2,5 hours with either free or liposomal fluorescent peptide (left) or protein (right). After washing, cells were fixated on the indicated time points and antigen loading was analyzed by flow cytometry. Data shown as geometric mean of NBD (left) or alexa647 (right) positive cells.

3.3.4 Liposomal antigen facilitates prolonged epitope presentation by DCs

Antigen presentation of the stored peptide antigen was studied by culturing the loaded DCs up to 72 hours post loading. At 24 hour time intervals the ability of DC to activate SIINFEKL-specific $CD8^+$ T-cells was determined. The DCs loaded with free peptide only activated SIINFEKL-specific $CD8^+$ T-cells directly after loading and overnight incubation (T= 0 hours), however, no more activation was observed 24 hours post 2.5 h pulse-incubation. In contrast, DCs incubated with cationic liposomal formulated peptide were still able to activate the SIINFEKL specific $CD8^+$ T-cells up to 72 hours post loading and incubation, indication enhanced sustained storage of liposome formulated antigen.

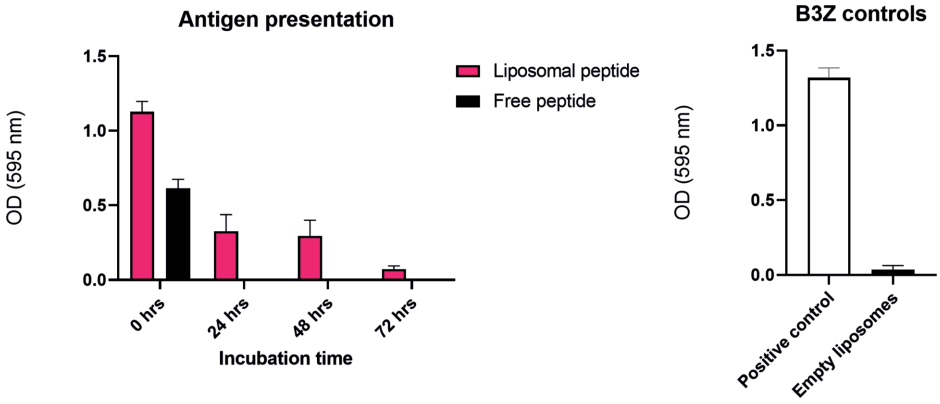

Figure 9. Sustained antigen presentation by dendritic cells. Activation of SIINFEKL-specific $CD8^+$ T-cells by mouse DCs loaded with either free or liposomal SIINFEKL containing long synthetic peptide (2 μM). Cells were incubated for 2.5 hours with the indicated compounds, next cells were washed and cultured during the indicated time periods. SIINFEKL-specific CD^+8 T-cells were incubated overnight with the DCs to determined specific antigen presentation. The OVA8 peptide containing the SIINFEKL minimal epitope served as a positive control (100 ng/ml in PBS) and empty liposomes as the negative control. Data shown as mean ± SEM (n=3) OD = optical density.

DISCUSSION

Cationic liposomes have shown to induce strong and effective T-cell responses in a wide variety of vaccines and are therefore of particular interest for cancer vaccines (1-4, 15, 32). In this work we explored the pharmaceutical and immunological mechanisms that contribute to efficient priming of antigen specific $CD8^+$ T-cells upon i.d. administered of peptide-loaded cationic liposomes.

Both the cationic liposomes and the encapsulated peptide were detectable at the SOI up to 2 weeks post vaccination, while neutral and anionic liposomes and the loaded lipopeptide were not detectable after 7 and 4 days respectively. The prolonged deposition at the SOI of the cationic liposomes most likely results from the interaction with a variety of (macro)molecules (e.g., proteins, lipids, sugars) present in the biological fluid upon injection (1, 17, 35). This interaction results in the coating of the liposomal surface and a so-called protein corona, resulting in alterations of liposomal physicochemical characteristics that can result in particle aggregation (17, 36-39). In various studies the deposition of cationic nanoparticles has been observed for the subcutaneous route and intramuscular route as well and was dependent on the cationic nature of the nanoparticles (1, 40). In this work we show that retention time at the SOI decreased when the zeta-potential is reduced (cationic > neutral > anionic), indicating that electrostatic interactions in-between anionic (macro)molecules and the positively charged liposomal surface could be a driving force in the depot formation.

The prolonged liposome and peptide presence at the SOI can contribute to improved $CD8^+$ T-cell priming as shown in this study. The formed depot allowed prolonged antigen presence at SOI and can facilitate continuous uptake of both antigen and liposomes by DCs that engulf the injection site. Additionally, there can be sustained draining of the peptide loaded liposomes to the lymph nodes where the nanoparticles are taken up by DCs and T-cell priming takes place (14, 17, 40-43). In order to further unravel the routing of the liposomes to the lymph nodes, either transport by DCs/APCs or direct draining, further imaging studies should be conducted. The most efficient priming was observed for peptide-loaded cationic liposomes and, interestingly, this formulation had the longest retention at the SOI for both peptide and liposomes. Admixing of peptide with empty cationic liposomes did induce antigen specific $CD8^+$ T-cell priming, however, not as much as encapsulated peptide, indicating different draining and/or transportation kinetics from the formed depot. The dissociation of peptide and liposomes can result in separate uptake of peptide and cationic liposome by DCs, resulting in inefficient $CD8^+$ T-cell priming (1-4, 32). In a different study similar observations were made for cationic nanoparticles in which encapsulated antigen outperformed particles admixed with antigen (44).

In addition, we explored the antigen handling by dendritic cells after engulfment of the cationic nanoparticles. Increased uptake of positively charged liposomes has been reported for multiple cell types and a possible explanation is the interaction between the negatively charged cell membrane and cationic liposomes (1, 11, 45). However, the protein corona also has an influence on nanoparticle uptake and can enhance receptor mediated uptake (37, 39, 46-50). Upon uptake our data suggest the intracellular storage of peptide loaded cationic liposomes similar to our previously published work with other antigen delivery systems like FcR, TLR and CLR targeted systems. A similar trend of sustained presence and antigen presentation capacity in MHC class I was observed for both peptide antigen formulated in cationic liposomes up to 72 hours post uptake. These results suggest that uptake of cationic liposomes by DCs is very efficient and are likely stored in mild endolysosomal compartments to sustain a continuous supply of antigenic peptides to MHC class I molecules. Future studies of more in-depth tracking of both antigen and liposomes upon uptake are required to determine intracellular handling of cationic nanoparticles by DCs. Additionally, comparison of multiple positively charged lipids would allow for identification of DOTAP specific effects on immune cell activation.

Altogether our data and published observation suggest that retention at the SOI, improved uptake, and sustained antigen storage contribute to the superior characteristics of cationic liposomes to achieve specific T-cell immunity.

CONCLUSION

Cationic liposomes mediate depot formation upon i.d. vaccination, prolonging peptide retention at the SOI and facilitate continous antigen presentation by DCs. The encapsulation of peptide in cationic liposomes induced more potent antigen specific $CD8^+$ T-cell compared to admixing and could be detected longer at the SOI. Neutral and anionic peptide loaded liposomes were cleared relatively quick from the SOI and did not induce antigen specific $CD8^+$ T-cells. These results indicate a significant advantage of cationic charge and form the basis for further exploration of immunological mechanisms of action of cationic liposome-based T-cell vaccines.

REFERENCES

1. Heuts J, Jiskoot W, Ossendorp F, van der Maaden K. Cationic Nanoparticle-Based Cancer Vaccines. Pharmaceutics. 2021;13(5).
2. Heuts J, Varypataki EM, van der Maaden K, Romeijn S, Drijfhout JW, van Scheltinga AT, et al. Cationic Liposomes: A Flexible Vaccine Delivery System for Physicochemically Diverse Antigenic Peptides. Pharm Res. 2018;35(11):207.
3. Varypataki EM, Benne N, Bouwstra J, Jiskoot W, Ossendorp F. Efficient Eradication of Established Tumors in Mice with Cationic Liposome-Based Synthetic Long-Peptide Vaccines. Cancer Immunol Res. 2017;5(3):222-33.
4. Varypataki EM, van der Maaden K, Bouwstra J, Ossendorp F, Jiskoot W. Cationic liposomes loaded with a synthetic long peptide and poly(I:C): a defined adjuvanted vaccine for induction of antigen-specific T cell cytotoxicity. AAPS J. 2015;17(1):216-26.
5. Korsholm KS, Hansen J, Karlsen K, Filskov J, Mikkelsen M, Lindenstrom T, et al. Induction of CD8+ T-cell responses against subunit antigens by the novel cationic liposomal CAF09 adjuvant. Vaccine. 2014;32(31):3927-35.
6. Hansen J, Lindenstrom T, Lindberg-Levin J, Aagaard C, Andersen P, Agger EM. CAF05: cationic liposomes that incorporate synthetic cord factor and poly(I:C) induce CTL immunity and reduce tumor burden in mice. Cancer Immunol Immunother. 2012;61(6):893-903.
7. Ma Y, Zhuang Y, Xie X, Wang C, Wang F, Zhou D, et al. The role of surface charge density in cationic liposome-promoted dendritic cell maturation and vaccine-induced immune responses. Nanoscale. 2011;3(5):2307-14.
8. Yan W, Chen W, Huang L. Reactive oxygen species play a central role in the activity of cationic liposome based cancer vaccine. J Control Release. 2008;130(1):22-8.
9. Vangasseri DP, Cui Z, Chen W, Hokey DA, Falo LD, Jr., Huang L. Immunostimulation of dendritic cells by cationic liposomes. Mol Membr Biol. 2006;23(5):385-95.
10. Le MQ, Carpentier R, Lantier I, Ducournau C, Fasquelle F, Dimier-Poisson I, et al. Protein delivery by porous cationic maltodextrin-based nanoparticles into nasal mucosal cells: Comparison with cationic or anionic nanoparticles. Int J Pharm X. 2019;1:100001.
11. Foged C, Brodin B, Frokjaer S, Sundblad A. Particle size and surface charge affect particle uptake by human dendritic cells in an in vitro model. Int J Pharm. 2005;298(2):315-22.
12. Thiele L, Rothen-Rutishauser B, Jilek S, Wunderli-Allenspach H, Merkle HP, Walter E. Evaluation of particle uptake in human blood monocyte-derived cells in vitro. Does phagocytosis activity of dendritic cells measure up with macrophages? J Control Release. 2001;76(1-2):59-71.
13. Thiele L, Merkle HP, Walter E. Phagocytosis and Phagosomal Fate of Surface-Modified Microparticles in Dendritic Cells and Macrophages. Pharmaceutical Research. 2003;20(2):221-8.
14. Schmidt ST, Olsen CL, Franzyk H, Worzner K, Korsholm KS, Rades T, et al. Comparison of two different PEGylation strategies for the liposomal adjuvant CAF09: Towards induction of CTL responses upon subcutaneous vaccine administration. Eur J Pharm Biopharm. 2019;140:29-39.
15. Pedersen GK, Andersen P, Christensen D. Immunocorrelates of CAF family adjuvants. Semin Immunol. 2018;39:4-13.
16. Henriksen-Lacey M, Christensen D, Bramwell VW, Lindenstrøm T, Agger EM, Andersen P, et al. Comparison of the depot effect and immunogenicity of liposomes based on dimethyldioctadecylammonium (DDA), 3β-[N-(N',N'-Dimethylaminoethane)carbomyl] cholesterol (DC-Chol), and 1,2-Dioleoyl-3-trimethylammonium propane (DOTAP): prolonged liposome retention mediates stronger Th1 responses. Mol Pharm. 2011;8(1):153-61.
17. Henriksen-Lacey M, Bramwell VW, Christensen D, Agger EM, Andersen P, Perrie Y. Liposomes based on dimethyldioctadecylammonium promote a depot effect and enhance immunogenicity of soluble antigen. J Control Release. 2010;142(2):180-6.

18. Kaur R, Bramwell VW, Kirby DJ, Perrie Y. Manipulation of the surface pegylation in combination with reduced vesicle size of cationic liposomal adjuvants modifies their clearance kinetics from the injection site, and the rate and type of T cell response. J Control Release. 2012;164(3):331-7.
19. Sahin U, Türeci Ö. Personalized vaccines for cancer immunotherapy. Science. 2018;359(6382):1355-60.
20. Vyas JM, Van der Veen AG, Ploegh HL. The known unknowns of antigen processing and presentation. Nat Rev Immunol. 2008;8(8):607-18.
21. Sanchez-Paulete AR, Teijeira A, Cueto FJ, Garasa S, Perez-Gracia JL, Sanchez-Arraez A, et al. Antigen cross-presentation and T-cell cross-priming in cancer immunology and immunotherapy. Ann Oncol. 2017;28(suppl_12):xii44-xii55.
22. Fehres CM, Unger WW, Garcia-Vallejo JJ, van Kooyk Y. Understanding the biology of antigen cross-presentation for the design of vaccines against cancer. Front Immunol. 2014;5:149.
23. van Montfoort N, Camps MG, Khan S, Filippov DV, Weterings JJ, Griffith JM, et al. Antigen storage compartments in mature dendritic cells facilitate prolonged cytotoxic T lymphocyte cross-priming capacity. Proc Natl Acad Sci U S A. 2009;106(16):6730-5.
24. Kloetzel PM, Ossendorp F. Proteasome and peptidase function in MHC-class-I-mediated antigen presentation. Current opinion in immunology. 2004;16(1):Curr Opin Immunol76-81.
25. Gao J, Ochyl LJ, Yang E, Moon JJ. Cationic liposomes promote antigen cross-presentation in dendritic cells by alkalizing the lysosomal pH and limiting the degradation of antigens. Int J Nanomedicine. 2017;12:1251-64.
26. Lonez C, Vandenbranden M, Ruysschaert JM. Cationic lipids activate intracellular signaling pathways. Adv Drug Deliv Rev. 2012;64(15):1749-58.
27. Lonez C, Lensink MF, Vandenbranden M, Ruysschaert JM. Cationic lipids activate cellular cascades. Which receptors are involved? Biochim Biophys Acta. 2009;1790(6):425-30.
28. Lonez C, Vandenbranden M, Ruysschaert JM. Cationic liposomal lipids: from gene carriers to cell signaling. Prog Lipid Res. 2008;47(5):340-7.
29. Ho NI, Camps MGM, de Haas EFE, Ossendorp F. Sustained cross-presentation capacity of murine splenic dendritic cell subsets in vivo. Eur J Immunol. 2018;48(7):1164-73.
30. Ho NI, Camps MG, Garcia-Vallejo JJ, Bos E, Koster AJ, Verdoes M, et al. Distinct antigen uptake receptors route to the same storage compartments for cross-presentation in dendritic cells. Immunology. 2021;164(3):494-506.
31. Sanderson S, Shastri N. LacZ inducible, antigen/MHC-specific T cell hybrids. Int Immunol. 1994;6(3):369-76.
32. Varypataki EM, Silva AL, Barnier-Quer C, Collin N, Ossendorp F, Jiskoot W. Synthetic long peptide-based vaccine formulations for induction of cell mediated immunity: A comparative study of cationic liposomes and PLGA nanoparticles. J Control Release. 2016;226:98-106.
33. van der Maaden K, Heuts J, Camps M, Pontier M, Terwisscha van Scheltinga A, Jiskoot W, et al. Hollow microneedle-mediated micro-injections of a liposomal HPV E743-63 synthetic long peptide vaccine for efficient induction of cytotoxic and T-helper responses. J Control Release. 2018;269:347-54.
34. Pizzuto M, Bigey P, Lachages AM, Hoffmann C, Ruysschaert JM, Escriou V, et al. Cationic lipids as one-component vaccine adjuvants: A promising alternative to alum. J Control Release. 2018;287:67-77.
35. Henriksen-Lacey M, Christensen D, Bramwell VW, Lindenstrom T, Agger EM, Andersen P, et al. Liposomal cationic charge and antigen adsorption are important properties for the efficient deposition of antigen at the injection site and ability of the vaccine to induce a CMI response. J Control Release. 2010;145(2):102-8.
36. Zhuang Y, Ma Y, Wang C, Hai L, Yan C, Zhang Y, et al. PEGylated cationic liposomes robustly augment vaccine-induced immune responses: Role of lymphatic trafficking and biodistribution. J Control Release. 2012;159(1):135-42.
37. Cai R, Chen C. The Crown and the Scepter: Roles of the Protein Corona in Nanomedicine. Adv Mater. 2019;31(45):e1805740.

38. Vu VP, Gifford GB, Chen F, Benasutti H, Wang G, Groman EV, et al. Immunoglobulin deposition on biomolecule corona determines complement opsonization efficiency of preclinical and clinical nanoparticles. Nat Nanotechnol. 2019;14(3):260-8.
39. Monopoli MP, Walczyk D, Campbell A, Elia G, Lynch I, Bombelli FB, et al. Physical-chemical aspects of protein corona: relevance to in vitro and in vivo biological impacts of nanoparticles. J Am Chem Soc. 2011;133(8):2525-34.
40. Baharom F, Ramirez-Valdez RA, Tobin KKS, Yamane H, Dutertre C-A, Khalilnezhad A, et al. Intravenous nanoparticle vaccination generates stem-like TCF1+ neoantigen-specific CD8+ T cells. Nature Immunology. 2020.
41. Christensen D, Henriksen-Lacey M, Kamath AT, Lindenstrom T, Korsholm KS, Christensen JP, et al. A cationic vaccine adjuvant based on a saturated quaternary ammonium lipid have different in vivo distribution kinetics and display a distinct CD4 T cell-inducing capacity compared to its unsaturated analog. J Control Release. 2012;160(3):468-76.
42. Lou G, Anderluzzi G, Tandrup Schmidt S, Woods S, Gallorini S, Brazzoli M, et al. Delivery of self-amplifying mRNA vaccines by cationic lipid nanoparticles: The impact of cationic lipid selection. J Control Release. 2020.
43. Ludewig B, Barchiesi F, Pericin M, Zinkernagel RM, Hengartner H, Schwendener RA. In vivo antigen loading and activation of dendritic cells via a liposomal peptide vaccine mediates protective antiviral and anti-tumour immunity. Vaccine. 2000;19(1):23-32.
44. Liu L, Ma P, Wang H, Zhang C, Sun H, Wang C, et al. Immune responses to vaccines delivered by encapsulation into and/or adsorption onto cationic lipid-PLGA hybrid nanoparticles. J Control Release. 2016;225:230-9.
45. Pedroso de Lima MC, Simões S, Pires P, Faneca H, Düzgüneş N. Cationic lipid–DNA complexes in gene delivery: from biophysics to biological applications. Advanced Drug Delivery Reviews. 2001;47(2):277-94.
46. Onishchenko N, Tretiakova D, Vodovozova E. Spotlight on the protein corona of liposomes. Acta Biomaterialia. 2021;134:57-78.
47. Mikelez-Alonso I, Aires A, Cortajarena AL. Cancer Nano-Immunotherapy from the Injection to the Target: The Role of Protein Corona. Int J Mol Sci. 2020;21(2).
48. Giulimondi F, Digiacomo L, Pozzi D, Palchetti S, Vulpis E, Capriotti AL, et al. Interplay of protein corona and immune cells controls blood residency of liposomes. Nat Commun. 2019;10(1):3686.
49. Benne N, van Duijn J, Lozano Vigario F, Leboux RJT, van Veelen P, Kuiper J, et al. Anionic 1,2-distearoyl-sn-glycero-3-phosphoglycerol (DSPG) liposomes induce antigen-specific regulatory T cells and prevent atherosclerosis in mice. Journal of Controlled Release. 2018;291:135-46.
50. Caracciolo G, Pozzi D, Capriotti AL, Cavaliere C, Piovesana S, La Barbera G, et al. The liposome-protein corona in mice and humans and its implications for in vivo delivery. J Mater Chem B. 2014;2(42):7419-28.

SUPPLEMENTARY FIGURES

1. Purification of fluorescent DOPE

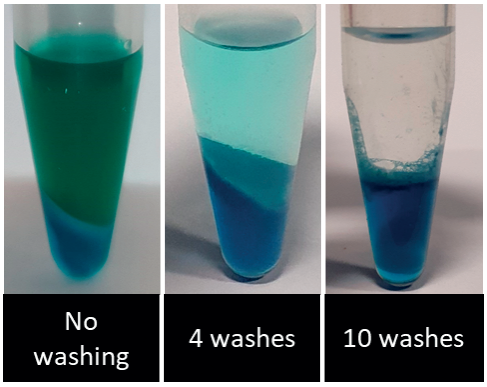

Supplemenrtary figure 1. Purification of fluorescent DOPE from the free near-infrared label IRdye-800CW-NHS by repeated Bligh-and-Dyer extractions.

2. Lipid and peptide content

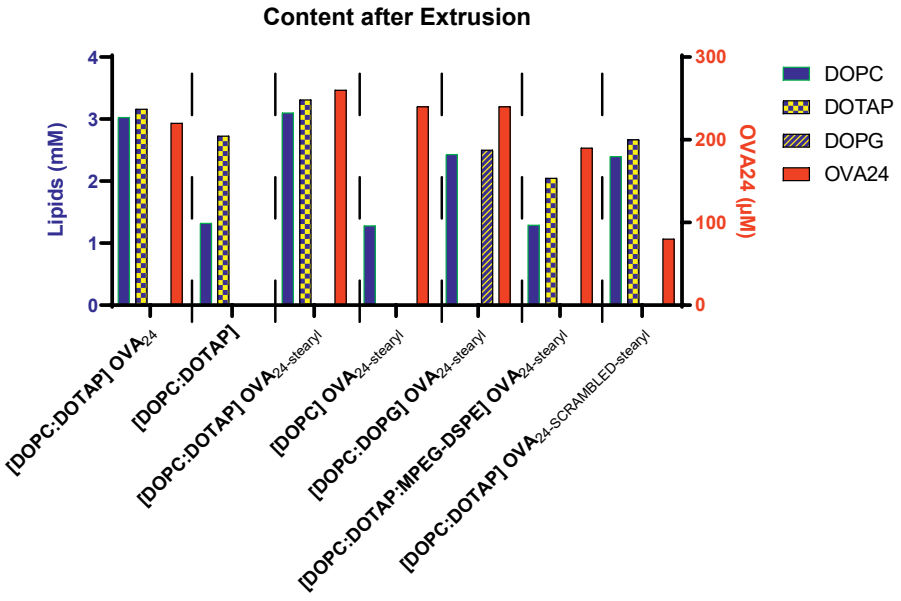

Supplementary figure 2. Lipid and peptide recovery of peptide loaded cationic, neutral and anionic liposomes.Peptide content was determined by UPLC-UV and lipid content by UPLC-ELSD (Heuts et al. submitted for publication).

3. Liposome stability upon storage

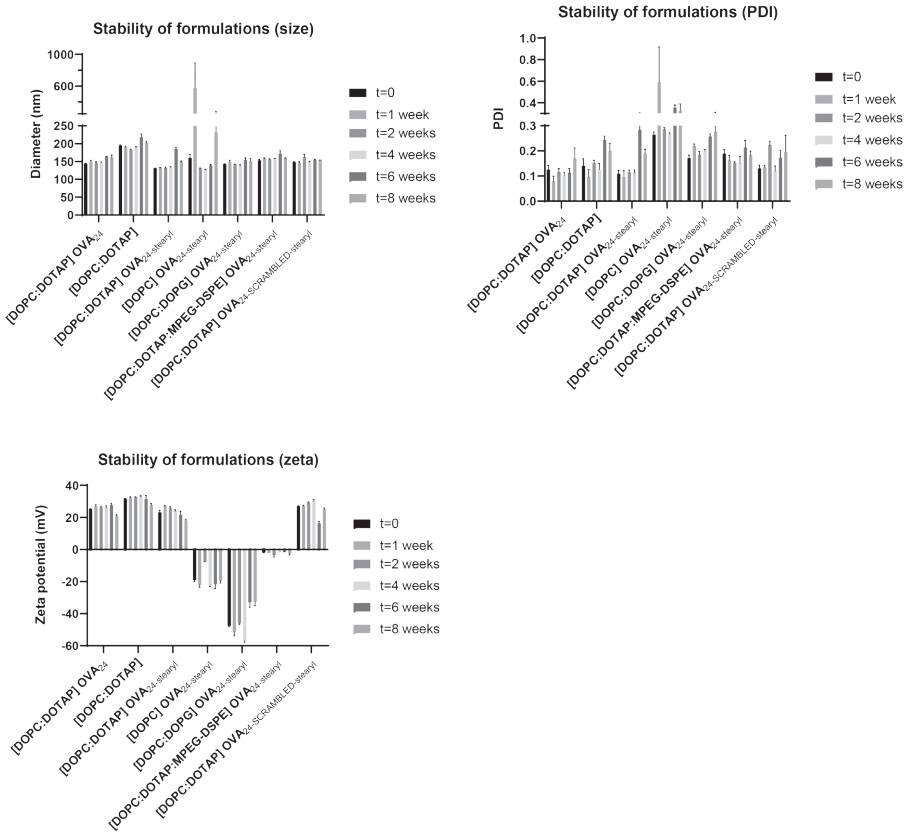

Supplementary figure 3 Physicochemical properties of the prepared empty, peptide and lipopeptide loaded liposomes throughout storage. The liposomes were stored during 8 weeks at 4°C. Every week the diameter and polydispersity index were determined by dynamic light scattering, and zeta potential by laser Doppler velocimetry. Data are displayed as average ± SD (n=3).

4. In vitro activation of CD8⁺ T-cell activation

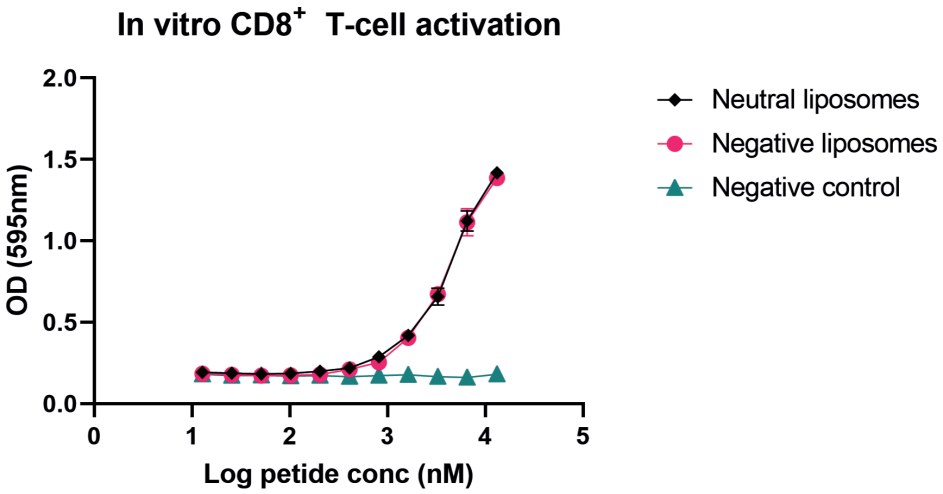

Supplementary figure 4. In vitro activation of the B3Z cells, SIINFEKL-specific hybridoma CD8⁺ T-cells, by DCs incubated with titrated amounts of lipopeptide loaded neutral and anionic liposomes. Data shown as mean ± SD (n=4).